MOMENTUM COMPACTION FACTOR MEASUREMENTS IN THE LARGE HADRON COLLIDER

J. Keintzel[*1], L. Malina, R. Tomás, 1211 CERN, Geneva 23, Switzerland
[1]also at Vienna University of Technology, 1040 Vienna, Austria

Abstract

The Large Hadron Collider (LHC) at CERN and its planned luminosity upgrade, the High Luminosity LHC (HL-LHC) demand well-controlled on- and off-momentum optics. Optics measurements are performed by analysing Turn-by-Turn (TbT) data of excited beams. Different techniques to measure the momentum compaction factor from these data are explored, taking into account the possibility to combine them with RF-voltage scans in future experiments.

INTRODUCTION

In circular machines, such as the Large Hadron Collider (LHC) [1] at CERN, particles with a momentum offset with respect to the reference momentum $\Delta p/p = \delta_p$ experience a different path length and hence a change of circumference with respect to on-momentum $\Delta C/C$. This relation is described by the momentum compaction factor α_C by

$$\alpha_C = \frac{\Delta C/C}{\delta_p} = \frac{I_1}{C} = \frac{1}{C} \oint \frac{\eta_x}{\rho} \, ds, \qquad (1)$$

with the horizontal dispersion η_x and the bending radius ρ. I_1 is the first synchrotron radiation integral. α_C enters in all momentum-dependent measurements such as dispersion or chromaticity and links transverse with longitudinal dynamics. In a perfect and flat machine α_C is given by the dispersion in the bending magnets, which itself is defined by quadrupole strengths. In the LHC α_C is typically between 3.2×10^{-4} and 3.5×10^{-4}. The phase slip factor η_C is defined with the relativistic gamma, $\gamma_{\rm rel}$, as $\eta_C = \gamma_{\rm rel}^{-2} - \alpha_C$.

α_C and η_C themselves depend also on δ_p, and hence it follows

$$\alpha_C = \sum_{i \geq 1} \alpha_C^{(i)} \delta_p^{i-1} \text{ and } \eta_C = \sum_{i \geq 1} \eta_C^{(i)} \delta_p^{i-1}, \qquad (2)$$

where the terms with $i = 1$ refer to the linear momentum compaction factor and the linear phase slip factor. The second-order momentum compaction factor, $\alpha_c^{(2)}$ can be calculated by [2, 3]

$$\alpha_C^{(2)} = \frac{1}{C} \oint \left(\frac{\eta'_x}{2} + \frac{\eta_x^{(2)}}{\rho} \right) ds, \qquad (3)$$

where $\eta'_x = d\eta_x/ds$. Although linear dispersion is measured routinely, the second-order dispersion $\eta_x^{(2)}$ has recently been measured for the first time for several optics in the LHC [4]. $\alpha_C^{(2)}$ can be controlled by sextupoles and can lead to an asymmetric momentum acceptance. In lepton machines such as in the FCC-ee [5] the design features such an asymmetric

momentum acceptance to account for the losses due to strong synchrotron radiation. In addition to a reduced momentum aperture, higher-order terms of the momentum compaction factor become more dominant for smaller $\alpha_C^{(1)}$ and can lead to smaller bucket sizes and enhancement of head-tail instability, where a detailed study can be found in [6, 7]. As $\alpha_C^{(2)}$ is generated by sextupoles, it is introduced by correcting the natural chromaticity. $\alpha_C^{(2)}$ hence depends on the horizontal tune Q_x and chromaticity $Q'_x = dQ_x/d\delta_p$ by [8]

$$\alpha_C^{(2)} = \frac{1 - 2Q'_x Q_x - Q_x^2}{Q_x^4} . \qquad (4)$$

$\alpha_C^{(2)}$ decreases for increasing Q_x and therefore with increasing machine circumference. For example, in the LHC $\alpha_C^{(2)}$ is approximately -3×10^{-4}, using Eq. (4), $Q_x = 62.31$ and $Q' = 2$. From Eq. (2) it follows that its contribution to the total momentum compaction factor is negligible, as the maximum momentum acceptance is about 6×10^{-4} [1]. Effects from second-order momentum compaction are therefore more dominant in machines where the natural tune is close to the matched chromaticity. The third order-momentum compaction factor, $\alpha_C^{(3)}$, is generated by, and can be controlled with octupoles. Recent studies showed that the momentum aperture can be symmetrically increased by optimizing octupole settings [3].

In the following different techniques to retrieve the momentum compaction factor, either from measurements of the transverse optics or the longitudinal one, are explored for several LHC optics of Run 2, together with prospects for future measurements.

TRANSVERSE OPTICS MEASUREMENTS

In the LHC optics of the horizontal and vertical plane are measured using Turn-by-Turn (TbT) beam position data. TbT measurements demand beam excitation, which can be performed with an AC-dipole [9]. Turn-by-Turn (TbT) orbit data is acquired at each Beam Position Monitor (BPM) [10] in SDDS [11] format. After data cleaning with algorithms based on SVD [12], harmonics analysis is performed with codes like HARPY [13, 14], where the output includes the measured closed orbit (CO) at each BPM. Together with the MAD-X [15] model horizontal dispersion $\eta_x^{\rm mdl}$ the relative momentum offset δ_p is typically calculated, using only arc BPMs, by

$$\delta_p = \frac{\langle \eta_x^{\rm mdl} CO_x \rangle}{\langle (\eta_x^{\rm mdl})^2 \rangle} . \qquad (5)$$

For off-momentum measurements δ_p are obtained for various relative frequency shifts. η_x is then retrieved from a

linear fit of CO_x over various δ_p at each BPM. It has to be noted that effects from second-order dispersion [4] are not included in Eq. (5). Optics measurements at 7 different fills at 6.5 TeV from 2016 and 2018 are used for the studies presented here, where more details on optics settings can be found in [4]. Optics measurements using TbT data depend on the model used and therefore the model momentum compaction factor enters indirectly in all obtained results.

Error Sources and Limitation

The calculation of δ_p relies on the model dispersion and the measured closed orbit. Great emphasis is therefore put into finding correct knob settings to reproduce measured crossing angles and beam separation in the model.

The measured closed orbit, however, is spoiled by BPM calibration errors. These can be estimated by comparing calibration independent optics measurements (β from phase advance [16, 17], normalised dispersion ($\eta/\sqrt{\beta}$) [18]) with calibration dependent results (β from amplitude [19], dispersion). In recent studies [20, 21] an average calibration error in the BPMs close to the interaction point of about 3 % with respect to the average calibration has been measured, where it has also been assumed that such uncertainties are not present in the arc BPMs.

As $\alpha_C^{(1)}$ depends on the quadrupole strengths, it is also affected by quadrupolar errors in the lattice, ΔK_1, which lead to a momentum compaction factor shift, of $\Delta\alpha_C = -\Delta K_1(\eta_x^2 - \eta_y^2)/C$ [7], with the vertical dispersion η_y. As $\eta_y^2 \ll \eta_x^2$ quadrupole errors at locations with large η_x are the main contributor to a change of the momentum compaction factor. As the linear momentum compaction depends in first order only on quadrupole fields in the machine, known normal and skew-quadrupole errors from 60 WISE tables [22, 23] are included in the bending dipoles, leading to 60 different machines. Before matching the tune and chromaticity to the measured values, corrections for the quadrupole errors are applied and the coupling is corrected using the closest tune approach. The rms β-beating with respect to the error free model results in approximately 2 % for analyzed optics. The resulting momentum compaction factor, $\alpha_C^{\text{mdl}+\Delta K_1}$, changes by less than 1 % with respect to the perfect model and is given in Table 1, where the errors represents the standard deviation over 60 seeds.

Beam Energy over Frequency

In synchrotrons devices such as a magnetic probe or a spectrometer can be installed to determine the beam energy, which is then used to evaluate the momentum compaction factor [24–26] at different RF-frequencies, which can be measured with great precision. In the LHC, however, no such device is presently installed, where recent investigations show the possibility to extract the beam energy from proton-ion operations [27]. The relative beam energy between different RF settings is equal to the relative momentum difference, computed from on- and off-momentum TbT measurements using Eq. (5). The momentum compaction factor

can then be measured using the relative frequency change, $\Delta f/f$, for various δ_p by

$$\delta_p = -\left(\frac{1}{\gamma_{\text{rel}}^{-2} + \alpha_C}\right)\frac{\Delta f}{f} . \tag{6}$$

As $\gamma_{\text{rel}}^{-2} \approx 10^{-8}$ for collision energy of 6.5 TeV it is negligible. As expected, a linear dependence of δ_p over $\Delta f/f$ is found, where an example is shown in Fig. 1 for an ATS [28] optics measurement. The relative difference between measured momentum compaction factors, σ^{fit}, and the model ones, which includes known quadrupole errors, $\alpha_C^{\text{mdl}+\Delta K_1}$ for all analyzed measurements is about (-2.95 ± 0.003) %, obtained by a least-square fit as shown in Fig. 2. Contrarily to previous studies [20, 21] the measured error of -3 % is therefore attributed to calibration errors in arc BPMs. Results for measured α_C^{fit} and resulting σ^{fit} are summarized in Table 1.
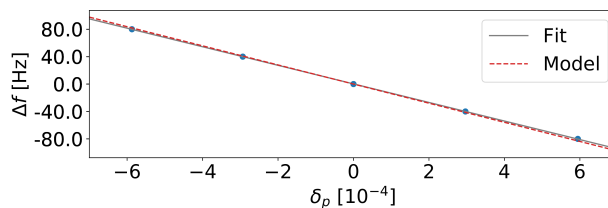

Figure 1: Relative momentum offset δ_p for relative change of RF-frequencies Δf for an ATS proton optics, obtained at 3rd October 2016.
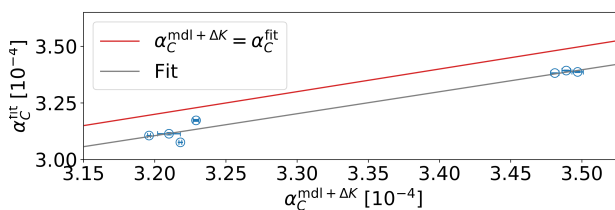

Figure 2: Measured momentum compaction factor obtained from fit, α_C^{fit}, over model momentum compaction factor including known qadrupole errors, $\alpha_C^{\text{mdl}+\Delta K_1}$.

Approximation with Dispersion

I_1 from Eq. (1) is only non zero in the bending dipoles. With measurements, however, the optics is only retrieved at the BPMs, where $I_1 = 0$. An approximation of I_1 can therefore be defined as $I_1 = \oint \frac{\eta_x}{\rho}\text{d}s \approx \langle\eta_x\rangle 2\pi$, where $\langle\eta_x\rangle$ refers to the average measured dispersion in the BPMs. The approximation of the momentum compaction factor, $\alpha_C^{\text{ap.}}$, therefore reads

$$\alpha_C \approx \alpha_C^{\text{ap.}} = \frac{2\pi\langle\eta_x\rangle}{C} . \tag{7}$$

By using this approximation a systematic error between α_C and $\alpha_C^{\text{ap.}}$ is introduced. The relative difference between the ideal model value, α_C^{mdl}, and the approximation used

Table 1: Model and Measured Momentum Compaction Factors for Different Optics. All momentum compaction factors are given in 10^{-4}. α_C^{mdl}: Ideal model. $\alpha_C^{\text{mdl}+\Delta K_1}$: Model including known quadrupole errors. $\alpha_C^{\text{mdl}+\Delta K,\text{ap.}}$: Model approximation using Eq. (7). α_C^{fit}: Measurement using fit of δ_p over $\Delta f/f$. σ^{fit}: Relative error between α_C^{fit} and $\alpha_C^{\text{mdl}+\Delta K_1}$. $\alpha_C^{\text{ap.}}$: Measured approximation using Eq. (7). $\sigma^{\text{ap.}}$: Relative error between $\alpha_C^{\text{ap.}}$ and $\alpha_C^{\text{mdl}+\Delta K,\text{ap.}}$. More information regarding measurement settings can be found in [4].

Date	Type	β^* [m]	Model			Measurements			
			α_C^{mdl}	$\alpha_C^{\text{mdl}+\Delta K_1}$	$\alpha_C^{\text{mdl}+\Delta K,\text{ap.}}$	α_C^{fit}	σ^{fit} [%]	$\alpha_C^{\text{ap.}}$	$\sigma^{\text{ap.}}$ [%]
26/03/16	physics	11	3.22	3.22 ± 0.001	3.28 ± 0.008	3.08 ± 0.001	-4.4	3.28	0.01
05/10/16	VdM	19.2	3.20	3.21 ± 0.008	3.26 ± 0.002	3.11 ± 0.010	-3.0	3.28	0.6
06/16/16	high β^*	2500	3.18	3.20 ± 0.001	3.26 ± 0.001	3.11 ± 0.001	-2.8	3.26	0.1
28/07/16	ATS	0.4	3.49	3.48 ± 0.003	3.51 ± 0.002	3.38 ± 0.001	-2.8	3.51	-0.3
03/10/16	ATS	0.21	3.49	3.50 ± 0.004	3.56 ± 0.003	3.39 ± 0.003	-3.1	3.57	0.1
16/10/16	ions	0.6	3.21	3.23 ± 0.002	3.29 ± 0.002	3.17 ± 0.005	-1.8	3.32	+1.4
03/11/18	ions	0.5	3.49	3.49 ± 0.003	3.54 ± 0.004	3.39 ± 0.002	-2.8	3.53	-0.4

in Eq. (7) and including errors, $\alpha_C^{\text{mdl}+\Delta K,\text{ap.}}$, is about +2 %, using only BPMs, which have not been cleaned in the dispersion measurement. Obtained measurement results from Eq. (7), $\alpha_C^{\text{ap.}}$, agree with the model expectation for analyzed samples with a relative difference, $\sigma^{\text{ap.}}$, typically below 1 %. This method can therefore neither be used to retrieve information about BPM calibration, nor the momentum compaction factor in the machine. This small $\sigma^{\text{ap.}}$ can result from not included field or misalignment errors. A summary of $\alpha_C^{\text{ap.}}$ and $\sigma^{\text{ap.}}$ for analyzed measurements is also given in Table 1.

MEASUREMENTS FROM LONGITUDINAL PARAMETERS

Complementary to transverse optics measurements, studies of longitudinal parameters can be performed to measure the momentum compaction factor. The phase slip factor can be measured by fitting the measured synchrotron tune Q_s over various RF-cavity voltages by [29]

$$Q_s^2 = \frac{h\eta_C qV \cos\varphi}{2\pi\beta_{\text{rel}}cp} , \tag{8}$$

with the harmonic number h, the unit charge q, the synchronous phase angle φ, the relativistic β_{rel}, the speed of light c and the particle momentum p. One difficulty in extracting the momentum compaction factor from RF-voltage scans in the LHC is that 16 RF-cavities are installed and the accuracy of determining the total change in V needs to be evaluated. Moreover, the synchronous phase itself also depends on V [29]. In other machines, such as in LEP, α_C has been measured using this method with a precision better than 10^{-3} [30]. Another option envisaged to be performed in future studies is by using the bunch length σ_z, the Q_s and the rms energy spread σ_E to fit the momentum compaction factor by

$$\sigma_z = \frac{c\sigma_\delta(\alpha_c - \gamma_{\text{rel}}^{-2})}{2\pi Q_s f_{\text{rev}}} , \tag{9}$$

with the revolution frequency f_{rev}. γ_{rel}^{-2} decreases from about 10^{-6} to 10^{-8} from 450 GeV injection energy to 6.5 TeV col-

lision energy. Neglecting this energy dependence therefore limits the precision of obtained α_c to 10^{-5} and 10^{-7}, respectively at injection and collision. Both methods are proposed to be used int the future for measuring momentum compaction.

SUMMARY AND OUTLOOK

Several options to measure the linear momentum compaction factor in the LHC have been explored. Transverse off-momentum optics measurements using TbT beam position data can be used to retrieve the momentum compaction and the BPM calibration by a fit of the relative change in RF-frequency over the relative momentum offset. By comparing measured momentum compaction with the model, including known quadrupolar errors, a relative error of approximately 3 % is found, which could result from calibration errors in arc BPMs. Re-analyzing statistically TbT measurements of previous runs and performing measurements with a LHC optics, which provides a factor 2 larger momentum compaction factor [31], could help clarifying BPM calibration in the LHC. The approximation of the momentum compaction using the dispersion agrees almost perfectly with the model, as information of BPM calibration is lost due to re-normalization in the analysis process and is therefore not suitable to identify BPM calibration. As transverse optics measurements depend on the used model, future studies to measure the momentum compaction factor and the phase slip factor from longitudinal parameters can be performed. Performing RF-voltage scans, envisaged to be tested in future runs, while measuring the synchrotron tune and the bunch length would allow to obtain the momentum compaction factor.

ACKNOWLEDGMENTS

REFERENCES

[1] O. Brüning *et al.*, "LHC Design Report", CERN, Geneva, Switzerland, Rep. No. CERN-2004-003-V-1, 2004.

[2] J.-P. Delahaye and J.Jäger, "Variation of the Dispersion Function, Momentum Compaction Factor, and Damping Partition Numbers with Particle Energy Deviation", *Part. Accel.*, vol. 18, pp. 183–201, 1986.

[3] M. Ries, "Nonlinear Momentum Compaction and Coherent Synchrotron Radiation at the Metrology Light Source", Ph.D. thesis, Humboldt University, Berlin, 2013.

[4] J. Keintzel *et al.*, "Second Order Dispersion Measurements in LHC", in *Proc. IPAC'19*, Melbourne, Australia, May 2019, pp. 496–500. doi:10.18429/JACoW-IPAC2019-MOPMP027

[5] A. Abada, M. Abbrescia, *et al.*, "FCC-ee: The Lepton Collider", *Eur. Phys. J. Spec. Top.*, vol. 228, p. 261, 2019. doi:10.1140/epjst/e2019-900045-4

[6] N.Y. Ng, "Small-Amplitude Synchrotron Tune near Transition ", FNAL, Batavia, IL, USA, Rep. Fermilab-0852-AD, 2010.

[7] A. W. Chao, K. H. Mess, M. Tigner, and F. Zimmermann, *Handbook of Accelerator Physics and Engineering*. Second edition, Singapore: World Scientific, 2013.

[8] F. Schmidt, P. Skowronski, V. Lebedev, and A. Valishev, "Higher Order Dispersion and Momentum Compaction in MAD-X/PTC Using Normal Form", CERN, Geneva, Switzerland, Rep. No. CERN-ACC-NOTE-2018-0062, 2018.

[9] M. Bai *et al.*, "Overcoming Intrinsic Spin Resonances with an RF Dipole", *Phys. Rev. Lett.*, vol. 80, p. 4673, 1998. doi:10.1103/PhysRevLett.80.4673

[10] R. Tomás, M. Aiba, A. Franchi, and U. Iriso, "Review of Linear Optics Measurement and Correction for Charged Particle Accelerators", *Phys. Rev. Accel. Beams*, vol. 20, p. 054801, 2017. doi:10.1103/PhysRevAccelBeams.20.054801

[11] M. Borland, L. Emery, H. Shang, and R. Soliday, "User's Guide for SDDS Toolkit Version 3.5.1". https://ops.aps.anl.gov/manuals/SDDStoolkit/SDDStoolkit.html

[12] R. Calaga and R. Tomás, "Statistical Analysis of RHIC Beam Position Monitors Performance", *Phys. Rev. Accel. Beams*, vol. 7, p. 042801, 2004. doi:10.1103/PhysRevSTAB.7.042801

[13] L. Malina, J. Coello de Portugal, J. Dilly, P. K. Skowroński, R. Tomás, and M. S. Toplis, "Performance Optimisation of Turn-by-Turn Beam Position Monitor Data Harmonic Analysis", in *Proc. IPAC'18*, Vancouver, Canada, Apr.-May 2018, pp. 3064–3067. doi:10.18429/JACoW-IPAC2018-THPAF045

[14] OMC3, https://github.com/pylhc/omc3

[15] MAD-X, https://mad.web.cern.ch/mad

[16] A. Wegscheider, A. Langer, R. Tomás, and A. Franchi, "Analytical *N* Beam Position Monitor Method", *Phys. Rev. Accel. Beams*, vol. 20, p. 11102, 2017. doi:10.1103/PhysRevAccelBeams.20.111002

[17] A. Langner *et al.*, "Utilizing the N Beam Position Monitor Method for Turn-by-Turn Optics Measurements", *Phys. Rev. Accel. Beams*, vol. 19, p. 092803, 2016. doi:10.1103/PhysRevAccelBeams.19.092803

[18] R. Calaga, R. Tomás, and F. Zimmermann, "BPM Calibration Independent LHC Optics Correction", in *Proc. PAC'07*, Albuquerque, NM, USA, Jun. 2007, paper THPAS091, pp. 3693–3695.

[19] P. Castro, "Luminosity and Beta Function Measurement at the Electron-positron Collider Ring LEP", Ph.D. thesis, Valencia University, 1996.

[20] A. García-Tabarés Valdivieso, "Optics Measurement Based Beam Position Monitor Calibration", Ph.D. thesis, Universidad Complutense de Madrid, Spain, 2019.

[21] A. García-Tabarés Valdivieso and R. Tomás, "Optics-Measurement-Based Beam Position Monitor Calibrations in the LHC Insertion Regions", *Phys. Rev. Accel. Beams*, vol. 23, p. 042801, 2020. doi:10.1103/PhysRevAccelBeams.23.042801

[22] P. Hagen *et al.*, "WISE: An Adaptive Simulation of the LHC Optics", in *Proc. EAPC'06*, Edinburgh, UK, Jun. 2006, paper WEPCH139, pp. 2248–2250.

[23] P. Hagen *et al.*, "WISE: A Simulation of the LHC Optics Including Magnet Geometrical Data", in *Proc. EAPC'08*, Genoa, Italy, Jun. 2008, paper TUPP091, pp. 1744–1746.

[24] J. Feikes and G. Wüstefeld, "Experimental Studies of the Nonlinear Momentum Compaction Factor at BESSY II", in *Proc. PAC'99*, New York, USA, Mar. 1999, pp. 2376–2378. doi:10.1109/PAC.1999.792696

[25] N. Carmignani, W. De Nolf, A. Franchi, Ch. J. Sahle, L. Torino, and B. Nash, "Measurement of the Momentum Compaction Factor of the ESRF Storage Ring", in *Proc. IPAC'19*, Melbourne, Australia, May 2019, pp. 1392–1395. doi:10.18429/JACoW-IPAC2019-TUPGW006

[26] A.-S. Müller, A. Ben Kalefa, I. Birkel, E. Huttel, F. Pérez, and M. Pont, "Momentum Compaction Factor and Nonlinear Dispersion at the ANKA Storage Ring", in *Proc. EPAC'04*, Lucerne, Switzerland, Jul. 2004, paper WEPLT068, pp. 2005–2007.

[27] E. Todesco and J. Wenninger, "Large Hadron Collider Momentum Calibration and Accuracy", *Phys. Rev. Accel. Beams*, vol. 20, p. 081003, 2017. doi:10.1103/PhysRevAccelBeams.20.081003

[28] S. Fartoukh, "Achromatic Telescopic Squeezing Scheme and Application to the LHC and its Luminosity Upgrade", *Phys. Rev. Accel. Beams*, vol. 16, p. 111002, 2013. doi:10.1103/PhysRevSTAB.16.111002

[29] M. Minty and F. Zimmermann, *Measurement and Control of Charged Particle Beams*. NY, USA: Springer Verlag Berlin Heidelberg, 2003.

[30] A.-S. Müller and J. Wenninger, "Synchrotron Tune and Beam Energy at LEP2", in *Proc. EPAC'00*, Vienna, Austria, Jun. 2000, paper MOP7B05, pp. 427–429.

[31] J. Keintzel, R. Tomás, R. Bruce, M. Giovannozzi, T. Risselada, and F. Zimmermann, "Lattice and Optics Options for Possible Energy Upgrades of the Large Hadron Collider", *Phys. Rev. Accel. Beams*, vol. 23, p. 101602, 2020. doi:10.1103/PhysRevAccelBeams.23.101602